10. *Npc1* cDNA from BALB/cStCrlfC3HfNctr $+^{npc}/+^{npc}$, BALB/cStCrlfC3HfNctr npc^{nih}/npc^{nih}, and C57BLKS/J *spm/spm* strains was isolated with primers mnpc1-3′ARev (5′-GAGAACAAGCTCTA-ATGAG-3′) and mp25-2R for reverse transcription of liver RNA and primer pairs mp25-1F/mnpc1-3′BREV (5′-GCCTACAACATTCTGAAGTCC-3′) and mp25-JF/mp25-3ASNB for PCR amplification in two segments. Three clones were analyzed for each strain by complete coverage sequencing.
11. Genomic intronic sequences of BALB/cStCrlf-C3HfNctr $+^{npc\text{-}nih}/+^{npc\text{-}nih}$ (GenBank accession number AF003349), BALB/cStCrlfC3HfNctr npc^{nih}/npc^{nih} (GenBank accession number AF003350), MaLR insertion event (GenBank accession number AF003351).
12. A. Cordonnier, J. F. Casella, T. Heidmann, *J. Virol.* **69**, 5890 (1995).
13. U. A. O. Heilein, R. Lange-Stablitzky, H. Schaal, W. Wille, *Nucleic Acids Res.* **14**, 6403 (1986); R. G. Kelly, *Genomics* **24**, 509 (1994); F. A. Smit, *Nucleic Acids Res.* **21**, 1863 (1993).
14. P. G. Pentchev, E. J. Blanchette-Mackie, E. A. Dawidowicz, *Trends Cell Biol.* **4**, 365 (1994).
15. The putative ORF begins at the first methionine of the longest ORF in the cDNA sequence. PSORT was used to predict signal peptide sequence {D. J. McGeogh, *Virus Res.* **3**, 271 (1985), modified by K. Nakai and M. Kanehisa [*Proteins Struct. Funct. Genet.* **11**, 95 (1991)]}. TM domains were predicted with PSORT [P. Klein, M. Kanehisha C. DeLisi, *Biochim. Biophys. Acta* **815**, 468 (1985)] and TMbase [K. Hoffman and W. Stoffel, *Biol. Chem. Hoppe-Seyler* **374**, 166 (1993)]. Putative TM domains 7, 10, and 11 predicted in the human NPC1 protein were not predicted by means of identical analyses with mouse NPC1. One of these TM domains is in the SSD region (*8*).
16. F. Letourneur and R. D. Klausner, *Cell* **69**, 1143 (1992); S. Ogata and M. Fukuda, *J. Biol. Chem.* **269**, 5210 (1994); W. Hunziker and H. J. Geuze, *BioEssays* **18**, 379 (1996).
17. D. G. Skalnik, H. Narita, C. Kent, R. D. Simoni, *J. Biol. Chem.* **263**, 6836 (1988); G. Gil, J. R. Faust, D. J. Chin, J. L. Goldstein, M. S. Brown, *Cell* **41**, 249 (1985).
18. X. Hua, A. Nohturfft, J. L. Goldstein, M. S. Brown, *Cell* **87**, 415 (1996).
19. R. L. Johnson *et al.*, *Science* **272**, 1668 (1996); L. V. Goodrich, R. L. Johnson, L. Milenkovic, J. A. McMahon, M. P. Scott, *Genes Dev.* **10**, 301 (1996).
20. J. Herz, T. E. Willnow, R. Farese Jr., *Nature Genet.* **15**, 123 (1997).
21. J. A. Porter, K. E. Young, P. A. Beachy, *Science* **274**, 255 (1996); J. A. Porter *et al.*, *Cell* **86**, 21 (1996); J. A. Porter *et al.*, *Nature* **374**, 363 (1995).
22. D. M. Stone *et al.*, *Nature* **384**, 129 (1996).
23. C. Chiang *et al.*, *ibid.* **383**, 407 (1996).
24. G. E. Homanics *et al.*, *Proc. Natl. Acad. Sci. U.S.A.* **90**, 2389 (1993); T. E. Willnow *et al.*, *ibid.* **93**, 8460 (1996); G. Salen *et al.*, *J. Lipid Res.* **37**, 1169 (1996).
25. Polymorphic carriers were generated by crossing BALB/cStCrlfC3HfNctr $npc^{nih}/+^{nih}$ animals to inbred (C57BL/6J) and WT-derived (CAST/Ei and MOLF/Ei) strains (Jackson Laboratory). F_1-carriers were identified by progeny testing offspring [P. G. Pentchev, R. O. Brady, A. E. Gal, S. R. Hibbert, *Biochim. Biophys. Acta* **488**, 312 (1977)]. An initial 736 meioses were typed [W. J. Pavan, S. Mac, M. Cheng, S. M. Tilghman, *Genome Res.* **5**, 29 (1995)] with markers *Umi 1* [A. J. Griffith *et al.*, *Mamm. Genome* **7**, 417 (1996)] *D18MIT64*, *D18MIT110*, and *D18MIT146* [http://www-genome.wi.mit.edu] to establish flanking markers *D18MIT64* and *D18MIT146*. For the remaining 816 meioses, only animals recombinant between flanking loci were genotyped with remaining loci and test-crossed to determine carrier status. Recombinant mice were from F_1-intercrosses, backcrosses to $npc^{nih}/+^{nih}$ carrier mice, and crosses with nonrecombinant F_2-carriers.
26. *Npc1* expression was detected by hybridization of a 1.7-kb PCR amplification product generated with primers 5′JF (5′-CTGTGTCCGAAATCCCACCTGC-3′) and 3′ASNB (5′-GTTAAATATCTGCTGCAC-CAGG-3′), representing nucleotides 1161 to 2901. AA002656 expression was detected with the excised 1-kb clone insert.
27. K. P. Dudov and R. P. Perry, *Cell* **37**, 457 (1984).
28. PCR primers mp25-8F (GGTGCTGGACAGCCAAG-TA) and mp25-INTR3 (5′-GATGGTCTGTTCTCCC-ATG-3′) flanking the insertion event were used to amplify the WT and mutant allele in Fig. 3D.
29. G. D. Schuler, S. F. Altschul, D. J. Lipman, *Proteins* **9**, 180 (1991).
30. We thank E. Neufeld, H. Varmus, D. Lipman, A. Wynshaw-Boris, L. Biesecker, R. Nussbaum, M. Meisler, and J. Trent for discussions and D. Leja for graphics. Supported by the Ara Parseghian Medical Research Foundation. Animal care was in accordance with NIH guidelines. This paper is dedicated to the memory of Michael Parseghian.

8 May 1997; accepted 5 June 1997

Abnormal Lignin in a Loblolly Pine Mutant

John Ralph,* John J. MacKay, Ronald D. Hatfield, David M. O'Malley, Ross W. Whetten, Ronald R. Sederoff

Novel lignin is formed in a mutant loblolly pine (*Pinus taeda* L.) severely depleted in cinnamyl alcohol dehydrogenase (E.C. 1.1.1.195), which converts coniferaldehyde to coniferyl alcohol, the primary lignin precursor in pines. Dihydroconiferyl alcohol, a monomer not normally associated with the lignin biosynthetic pathway, is the major component of the mutant's lignin, accounting for ~30 percent (versus ~3 percent in normal pine) of the units. The level of aldehydes, including new 2-methoxybenzaldehydes, is also increased. The mutant pines grew normally indicating that, even within a species, extensive variations in lignin composition need not disrupt the essential functions of lignin.

Lignins are complex phenolic plant polymers essential for mechanical support, defense, and water transport in vascular terrestrial plants (*1*, *2*). They are usually derived from three hydroxycinnamyl alcohol precursors **2a** through **c** in varying proportions (Fig. 1). In gymnosperms—for example, pine and other conifers—lignin is polymerized from only two of the three monomers, *p*-coumaryl alcohol **2a** and coniferyl alcohol **2b**, with coniferyl alcohol being predominant (~90%). *p*-Coumaryl alcohol–derived subunit levels are increased in compression wood, which forms during mechanical or gravitational stress and in wood knots (*3*). In woody angiosperms, lignin is derived from coniferyl alcohol **2b** and sinapyl alcohol **2c** in roughly equal proportions. Precursors and derivatives of hydroxycinnamyl alcohols also contribute to the lignin structure. For example, acetylated monolignols (hydroxycinnamyl acetates) have been implicated in kenaf (*Hibiscus cannabinus*) (*4*) and woody angiosperms (*5*), and *p*-coumarate esters are found in all grass lignins, implicating hydroxycinnamyl *p*-coumarates as precursors (*6*, *7*). Low levels (~5%) of cinnamaldehydes and benzaldehydes are present in all isolated lignins and are responsible for the bright crimson staining of lignified tissues by phloroglucinol-HCl (*8*).

Removal of lignin from wood and plant fibers is the basis of chemical pulping to produce diverse pulp and paper products. Genetic engineering of the lignin biosynthetic pathway to lower lignin concentration or construct lignins more amenable to extraction is an active area of current research (*9*). However, several mutations have been identified and characterized that affect the lignin biosynthetic pathway (*10*). In maize (*Zea mays*) and related grasses, mutants characterized by a brown midrib (*bm* or *bmr*) have modified lignin (*11*). The *bm* phenotype can result from changes affecting cinnamyl alcohol dehydrogenase (CAD) (for example, *bm1* of maize) (*12*, *13*), O-methyl transferase (OMT) (for example, *bm3* of maize) (*12*, *13*), or both CAD and OMT (for example, *bmr6* of sorghum, *Sorghum bicolor*) (*14*). Mutations in two other maize genes also result in brown midrib phenotypes, but the products of these genes remain unknown. A mutation in the gene encoding ferulate-5-hydroxylase has been identified in *Arabidopsis thaliana*, but it does not result in a brown midrib phenotype (*15*). No lignin mutants have been previously identified in woody plants.

CAD catalyzes the last step of the lignin precursor biosynthetic pathway (Fig. 1), reduction of hydroxycinnamaldehydes **1** to hydroxycinnamyl alcohols **2** (the conventional lignin monomers or monolignols) (*16*). A reduction in CAD activity might

J. Ralph, U.S. Dairy Forage Research Center, U.S. Department of Agriculture (USDA)–Agricultural Research Service (ARS), Madison, WI 53706–1108, and Department of Forestry, University of Wisconsin, Madison, WI 53706–1598, USA.
J. J. MacKay, Department of Genetics, North Carolina State University (NCSU), Raleigh, NC 27695–7614, USA.
R. D. Hatfield, U.S. Dairy Forage Research Center, USDA-ARS, Madison, WI 53706–1108, USA.
D. M. O'Malley and R. W. Whetten, Department of Forestry, NCSU, Raleigh, NC 27695–8008, USA.
R. R. Sederoff, Department of Genetics, NCSU, Raleigh, NC 27695–7614 and Department of Forestry, NCSU, Raleigh, NC 27695–8008, USA.

*To whom correspondence should be addressed at U.S. Dairy Forage Research Center, USDA-ARS, 1925 Linden Drive West, Madison, WI 53706–1108, USA. E-mail: jralph@facstaff.wisc.edu

lead to accumulation of hydroxycinnamaldehydes **1** that could copolymerize with normal lignin monomers. Transgenic plants, suppressed in the synthesis of CAD (*9*, *17*), sometimes have red-brown xylem tissue resembling that of grass brown midrib mutants. Such plants have increased aldehyde levels, although little of the aldehyde may actually be incorporated into the lignin (*9*, *17*). The molecular basis for the color has not been established, but higher order polymers of coniferaldehyde **1b**, synthesized in vitro, have a wine-red color (*18*).

Here we report that a viable loblolly pine, homozygous for the mutant *cad-n1* allele (*19*), incorporates novel monomers into its lignin in response to a CAD deficiency. The lignin structural changes were extensive and not predicted by the current view of the lignin biosynthetic pathway. The wood of this mutant is brown-red (Fig. 2), similar to the color of the xylem in *brown midrib* mutants (*11*) and transgenic plants suppressed in lignin biosynthetic enzyme activity (*9*, *17*). The *cad-n1* allele is inherited as a Mendelian recessive gene that maps to the same genomic region as the *cad* locus. The *cad-n1* allele was identified in a well-characterized heterozygous loblolly pine genotype (clone 7-56). In homozygous *cad-n1* plants, CAD activity is 1% or less of wild type, and relative abundance of *cad* mRNA transcript is greatly decreased. In mutant plants, free coniferaldehyde **1b** (the CAD substrate) accumulates to a high level. Unlike transgenic plants suppressed in CAD, *cad-n1* mutant seedlings have decreased lignin content (*19*).

Fig. 2. (Left) Wood chips from normal wood and a homozygous mutant with reduced CAD activity showing the brown wood phenotype. The mutant wood was obtained from a field test containing progeny from a cross between two half-sib loblolly pines each heterozygous for the mutant *cad* gene. (Right) Immediately after debarking, 2-year-old trees. The *cad-n1* mutant is readily identified by the red-brown color of its wood.

Milled wood lignins (*20*) were isolated for nuclear magnetic resonance (NMR) analysis from the wood of a 12-year-old CAD-deficient mutant and a normal sibling from the same cross (Fig. 2). An estimate of the subunit composition of this unusual lignin fraction, on the basis of quantitative NMR and other analytical data, is given in Table 1.

NMR spectra show that both coniferaldehyde **7** and vanillin **5** (*21*) end groups are present in the lignin of the pine mutant, as may be expected from the suppression of CAD. Wood from the mutant also had a higher extractable aldehydes content (*19*). The HMQC-TOCSY (heteronuclear multiple-quantum coherence–total correlation spectroscopy) spectrum reveals the side-chain coupling network in which protons 7, 8, and 9 correlate with the aldehyde carbonyl carbon, C-9 in **7** and the simple 1-bond correlation between C-7 and H-7 in **5** (Fig. 3). However, such components are also present in milled wood lignins from normal loblolly pine (Fig. 3). From quantitative NMR, these aldehydes each account for ~15% of mutant lignin units and ~7% in the normal pine lignin (Table 1). More striking are 2-methoxybenzaldehyde components **6** (*22*), the peaks at ~188 parts per million (ppm), that are greatly enhanced in the mutant (Fig. 3). The source of these previously unreported 2-methoxybenzaldehydes in lignins is unknown. Lignins from both the normal and mutant trees contained higher than normal concentrations of *p*-coumaryl alcohol units because of the preponderance of knots.

Dihydroconiferyl alcohol units **8** are present and predominant. The HMQC-TOCSY experiment (*23*) (Fig. 4) identified the coupling network for the aryl propanol side chain (red and orange contours) that is consistent with model compound data (*24*). Products **8a,b** (red) representing heterocoupling of dihydroconiferyl alcohol with a conventional lignin monomer or oligomer as well as dibenzodioxocins **8c** (orange) from initial 5-5-homo-coupling of dihydroconiferyl alcohol monomers are present in roughly equal amounts, reinforcing the claim that dihydroconiferyl alcohol is a major monomer during lignification.

Dihydroconiferyl alcohol products are seen in synthetic lignins that are prepared from impure monomers. The best syntheses of hydroxycinnamyl alcohols **2** (*25*) from

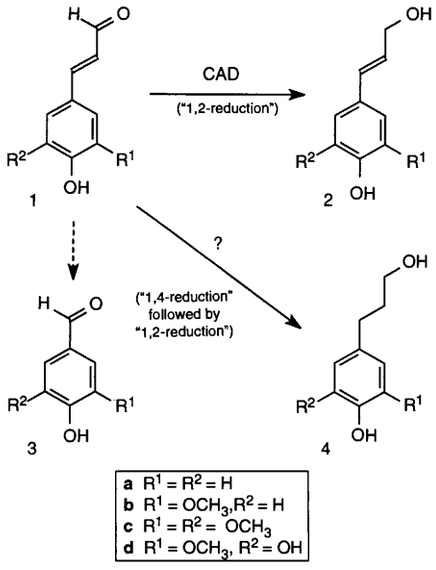

Fig. 1. Some precursors and products in the lignin biosynthetic pathway. The normal lignin monomers are the *p*-hydroxycinnamyl alcohols **2**; *p*-coumaryl alcohol **2a**, coniferyl alcohol **2b,** and sinapyl alcohol **2c**. Coniferaldehyde **1b** is normally reduced regioselectively to produce coniferyl alcohol **2b**. When CAD activity is depressed, coniferaldehyde **2b** accumulates and could polymerize or copolymerize into lignin. Dihydroconiferyl alcohol **4b**, observed previously only as a minor component of softwood lignins, is presumed to derive from coniferaldehyde **1b** via a 1,4-reduction followed by a 1,2-reduction. However, no mechanism for this conversion has been reported. *p*-Coumaryl alcohol **2a** is readily derived from its aldehyde **1a** in the mutant, implying that different CAD enzymes are involved for **1a**→**2a** versus **1b**→**2b**.

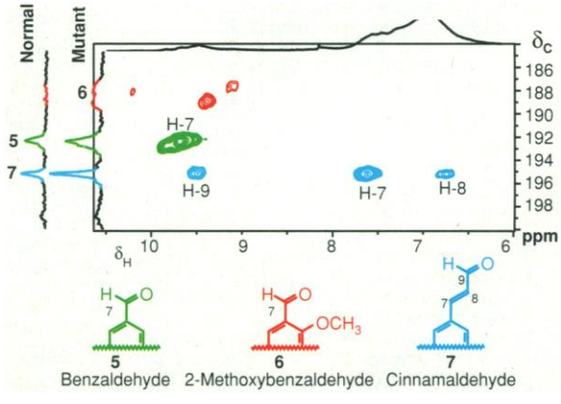

Fig. 3. Aldehyde carbonyl group correlations from the HMQC-TOCSY (*23*) spectrum of lignin from the *cad-n1* mutant plant showing the presence of cinnamaldehyde (with correlations to the three side-chain protons) and benzaldehyde (single correlations) units in the lignin. The normal pine lignin carbon section is shown to the left. The ^{13}C spectra shown on projections to the left of the figure are normalized to the same methoxyl level; cinnamaldehyde **7** and benzaldehyde **5** signals are about twice as abundant in the mutant. The higher field aldehydes markedly increased in the mutant have now been identified as 2-methoxybenzaldehydes **6** (*22*); their source is unknown.

hydroxycinnamate esters or hydroxycinnamaldehydes **1** still produce small amounts of 1,4-reduction products **4**. Purification of coniferyl alcohol is difficult because dihydroconiferyl alcohol cocrystalizes with it. A synthetic lignin prepared (*26*) from coniferyl alcohol **2b** containing a few percent dihydroconiferyl alcohol **4b** provides a convenient model for the lignin in the pine mutant. Its HMQC-TOCSY spectrum (Fig. 4C) shows the same dihydroconiferyl alcohol side-chain signals as in the pine lignins. A parallel between the lignins isolated from the mutant tree and hydride reduction product synthetic lignins is apparent. A small amount of the initial dihydroconiferyl alcohol homo-coupling product **8c** (orange) is seen in the spectrum of the synthetic lignin (Fig. 4C)—the saturated compound is quickly and efficiently dimerized via radical processes. Normal softwood lignins contain small amounts of dihydroconiferyl alcohol units (Fig. 4B). The source of these subunits is unknown. Although dihydroconiferyl alcohol and its glucoside have been detected in young plant tissues including pine (*27*) and may function as growth factors (*28*), they are not considered part of the normal lignin biosynthetic pathway.

CAD normally effects a regioselective "1,2-reduction" (at C-9) of coniferaldehyde **1b** to produce coniferyl alcohol **2b**. Our results suggest that the loss of CAD activity activates or up-regulates pathways on the basis of "1-4 reduction" (at C-7) and subsequent 1,2-reduction during lignin formation to produce the dihydroconiferyl alcohol monomer **4b** (Fig. 1). Analogously, synthetic preparation of coniferyl alcohol versus dihydroconiferyl alcohol can be selected by hydride reactions with 1,2- versus 1,4-regiochemistry (Fig. 1) (*25*). An alternative possibility is that a small structural change in the enzyme (for example, a disulfide bridge) affecting the active site of the CAD enzyme might be enough to provide the "hydride" equivalent to the 7-carbon site. This possibility is unlikely, and an alternative enzymatic activity is probably required because the relative abundance of steady-state *cad* mRNA transcripts is greatly decreased in the mutant, and the amount of CAD enzyme activity is reduced to ≤1% of wild type (*19*). If the biochemical reduc-

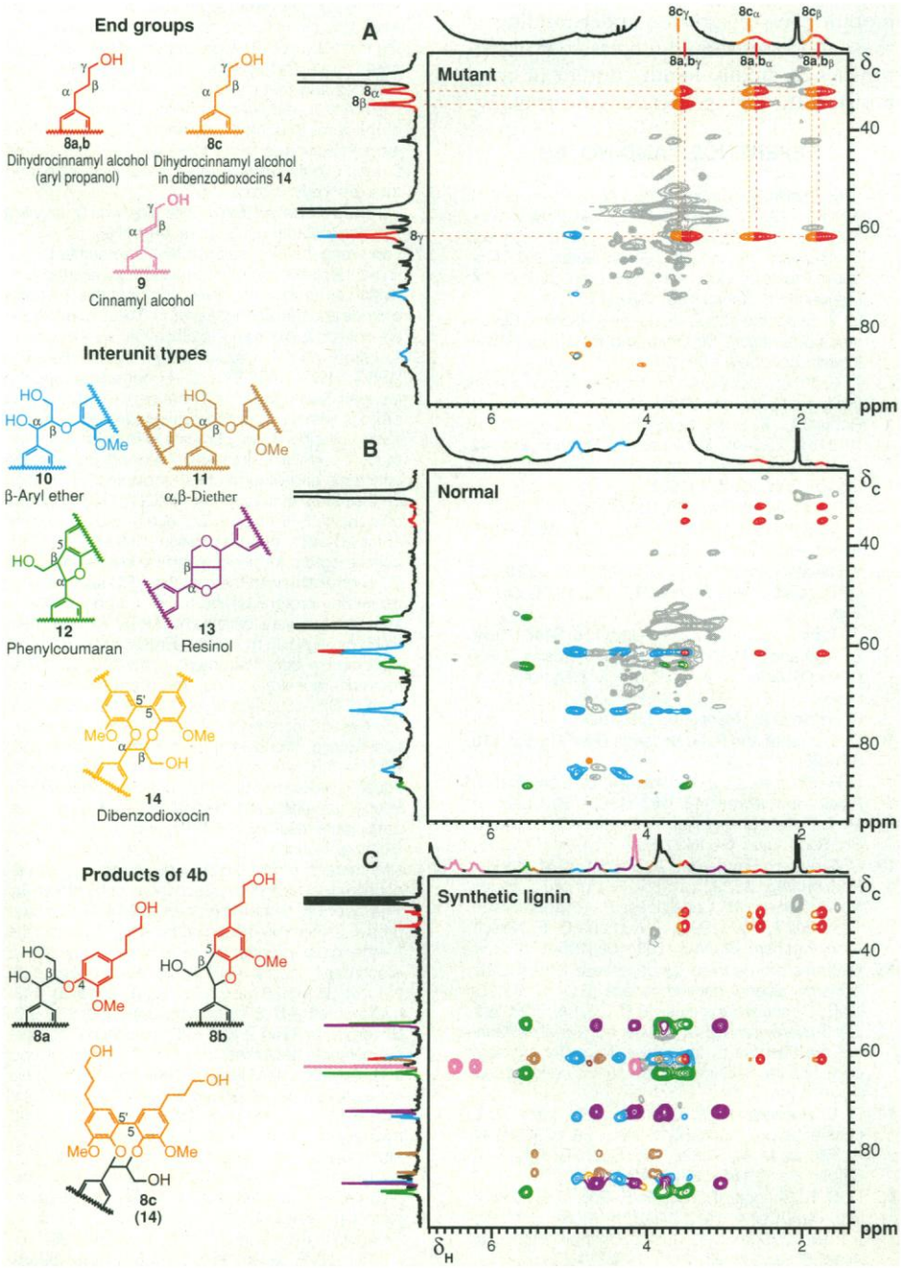

Fig. 4. Regions of the HMQC-TOCSY spectra (*23*) of milled wood lignins from (**A**) the pine *cad-n1* mutant, (**B**) from a *cad* normal wood, and (**C**) from a synthetic lignin (*26*). Structure assignments are most easily seen in spectrum (C) from the synthetic lignin that derived from coniferyl alcohol **2b** containing ~2% dihydroconiferyl alcohol **4b** (*26*). Although synthetic lignins of this type have quite different substructure ratios from plant lignins, they contain all of the structural units and are valuable for spectral assignment. Thus, in (C), β-aryl ether units **10**, α,β-diaryl ethers **11** (scarce in plant lignins), phenylcoumarans **12**, and resinols **13** are readily identified, along with coniferyl alcohol end groups **9** and the dihydroconiferyl alcohol units **8** (and the aldehyde units **5** and **7** in Fig. 3). Red- and orange-colored contours show the unambiguously identified components **8** arising from dihydroconiferyl alcohol monomers **4**. NMR provides a convenient distinction between products of hetero-coupling of **4** with conventional lignin monomers or oligomers to give **8a,b** (red) and those from initial 5-5-homo-coupling of dihydroconiferyl alcohol monomers to give **8c** (orange). Both are equally represented in the *cad-n1* mutant, whereas the normal pine has only the higher field component, and the synthetic lignin has a trace of the lower field component. NMR data from cross-coupled dimeric models for 4-*O*-β structures **8a** and 5-β/4-*O*-α (phenylcoumaran) structures **8b** and the dibenzodioxocin **8c** coincide with the lignin data observed here (*24*). In the CAD mutant, dihydroconiferyl units are dominant, displacing much of the intensity from the normal coniferyl alcohol–derived region. Some of the minor units can be seen in the pine samples when looking at lower contour levels (not shown). The normally predominant β-aryl ether (blue) and phenylcoumaran (green) components (B) are severely reduced in the *cad-n1* mutant, with only some β-ether peaks being observable at comparable contour levels—these may also arise from *p*-coumaryl alcohol (in addition to coniferyl alcohol). Gray contours are from intense methoxyl signals, carbohydrate impurities, and other lignin structures not discussed in this paper.

tion is not totally regioselective, the small amounts of **4b** producing the dihydroconiferyl units **8** seen in normal pine lignins could be explained, but this rationale would not allow production of **4b** in such major proportions without a significant shift in enzyme activity or without enhanced activity of an alternate enzyme. At least one new enzyme would be required to explain these results. It is also possible that coniferaldehyde is not the precursor to dihydroconiferyl alcohol, and that its synthesis is up-regulated from other sources in the plant.

The amount of subunits derived from *p*-coumaryl alcohol **2a** in the mutant is unchanged (Table 1), whereas the amount of coniferyl alcohol subunits **2b** is greatly reduced (*29*). These results imply that the formation of *p*-coumaryl alcohol **2a** uses an independent mechanism such as an additional enzyme with "1,2-reductase activity" specific for *p*-hydroxycinnamaldehyde **1a**. Furthermore, few dihydro-*p*-coumaryl alcohol **4a** units were detected (*29*). The 1,4-reductase activity proposed for the formation of dihydroconiferyl alcohol is therefore equally specific for coniferaldehyde **1b**.

Incorporation of novel monomers into lignin is inconsistent with the high level of enzymatic specificity recently extended to lignin formation from observations of specificity in lignin biosynthesis (*30*). Independence from rigid enzymatic control is further supported by other examples of incorporation of nontraditional monomers into lignins: (i) ferulates and diferulates actively incorporate into lignins of grasses, effecting significant lignin-polysaccharide cross-linking (*31*); (ii) acylated monomers are implicated in a variety of species (*4–7*); (iii) 5-hydroxyconiferyl alcohol **2d**-derived subunits are readily assimilated into a lignin polymer in OMT-deficient plants that have a reduced ability to produce sinapyl alcohol (*32*).

Table 1. Estimates of subunit compositions [from quantitative ^{13}C-NMR and DFRC (*29*) data] of the normal (*cad*) and mutant pine (*cad-n1*) isolated lignins. **2a**, *p*-coumaryl alcohol units; **2b**, coniferyl alcohol units; **1**, cinnamaldehyde units (*p*-hydroxycinnamaldehyde and coniferaldehyde units are not distinguished); **3**, benzaldehyde units (*p*-hydroxybenzaldehyde and vanillin units are not distinguished); (*) aldehydes at ~188 ppm in ^{13}C-NMR spectra are identified as 2-methoxybenzaldehydes **6** (*22*) from unknown sources—the other substituents on the aromatic ring are unknown; **4b**, dihydroconiferyl alcohol (+ traces of dihydro-*p*-coumaryl alcohol **4a**), the major component of the *cad-n1* mutant lignin.

Lignin	1	2a	2b	3	4b	*
cad-n1	15	10	15	15	30	15
cad	7	10	73	7	3	Trace

Well-characterized differences in lignin subunit composition have long been known between major taxonomic groups of higher plants—for example, between lignins of hardwood and softwood trees (*33*). However, the narrow range of variation in lignin compositions within groups (*10*) has suggested structural constraints imposed for vascular function and support. The ability of this pine mutant to produce a functional lignin polymer from unexpected subunits extends the limit of "metabolic plasticity" for the formation of lignin, within an individual species. Concepts of lignin function based on the previous range of lignin compositions must now be reexamined in view of the unusual structure and composition of lignin in this mutant pine. A greater understanding of these processes should increase our opportunities to modify lignin content or composition through genetic engineering.

REFERENCES AND NOTES

1. J. M. Harkin, in *Oxidative Coupling of Phenols*, W. I. Taylor and A. R. Battersby, Eds. (Dekker, New York, 1967), pp. 243–321; J. M. Harkin, in *Chemistry and Biochemistry of Herbage*, G. W. Butler, Ed. (Academic Press, London, 1973), vol. 1, pp. 323–373; K. Freudenberg, *Nature* **183**, 1152 (1959).
2. K. V. Sarkanen and C. H. Ludwig, *Lignins: Occurrence, Formation, Structure and Reactions* (Wiley-Interscience, New York, 1971).
3. T. E. Timell, *Compression Wood in Gymnosperms* (Springer-Verlag, New York, 1986); H. H. Nimz, D. Robert, O. Faix, M. Nemr, *Holzforschung* **35**, 16 (1981); C. Lapierre, B. Monties, C. Rolando, *ibid.* **42**, 409 (1988); K. Fukushima and N. Terashima, *Wood Sci. Technol.* **25**, 371 (1991).
4. J. Ralph, *J. Nat. Prod.* **59**, 341 (1996).
5. K. V. Sarkanen, H.-M. Chang, G. G. Allan, *Tech. Assoc. Pulp Pap. Ind.* **50**, 587 (1967).
6. Y. Nakamura and T. Higuchi, *Holzforschung* **30**, 187 (1976); *Cell. Chem. Technol.* **12**, 199 (1978); *ibid.*, p. 209.
7. J. Ralph *et al.*, *J. Am. Chem. Soc.* **116**, 9448 (1994).
8. E. Adler and L. R. Ellmer, *Acta Chem. Scand.* **2**, 839 (1948); E. Adler, K. J. Björkquist, S. Häggroth, *ibid.*, p. 93.
9. C. Halpin *et al.*, *Plant J.* **6**, 339 (1994).
10. M. Campbell and R. R. Sederoff, *Plant Physiol.* **110**, 3 (1996).
11. J. H. Cherney, D. J. R. Cherney, D. E. Akin, J. D. Axtell, *Adv. Agron.* **46**, 157 (1991); B. Chabbert, M. T. Tollier, B. Monties, Y. Barriere, O. Argiller, *J. Sci. Food Agric.* **64**, 349 (1994).
12. C. Grand, P. Parmentier, A. Boudet, A. M. Boudet, *Physiol. Veg.* **23**, 905 (1985); F. Vignols, J. Rigau, M. A. Torres, M. Capellades, P. Puigdomenech, *Plant Cell* **7**, 407 (1995); J. Kuc and O. E. Nelson, *Arch. Biochem. Biophys.* **105**, 103 (1964).
13. Enzymes are denoted by uppercase letters: CAD, cinnamyl alcohol dehydrogenase (E.C. 1.1.1.195); OMT, *O*-methyl transferase (E.C. 2.1.1.6); F5H, ferulate 5-hydroxylase (E.C. number not available). Gene loci are denoted by lowercase italics (for example, *cad*), and the CAD-deficient mutant is denoted *cad-n1*.
14. D. L. Bucholtz, R. P. Cantrell, J. D. Axtell, V. L. Lechtenberg, *J. Agric. Food Chem.* **28**, 1239 (1980); C. Pillonel, M. M. Mulder, J. J. Boon, B. Forster, A. Binder, *Planta* **185**, 538 (1991).
15. C. C. S. Chapple, T. Vogt, B. E. Ellis, C. R. Somerville, *Plant Cell* **4**, 1413 (1992); K. Meyer, J. C. Cusumano, C. Somerville, C. C. S. Chapple, *Proc. Natl. Acad. Sci. U.S.A.* **93**, 6869 (1996).
16. D. M. O'Malley, S. Porter, R. R. Sederoff, *Plant Physiol.* **98**, 1364 (1992).
17. T. Hibino, K. Takabe, T. Kawazu, D. Shibata, T. Higuchi, *Biosci. Biotechnol. Biochem.* **59**, 929 (1995); M. Baucher *et al.*, *Plant Physiol.* **112**, 1479 (1996).
18. T. Higuchi, T. Ito, T. Umezawa, T. Hibino, D. Shibata, *J. Biotechnol.* **37**, 151 (1994).
19. J. J. MacKay *et al.*, *Proc. Natl. Acad. Sci. U.S.A.*, in press; J. J. MacKay, thesis, North Carolina State University (1997).
20. Milled wood lignin [A. Björkman, *Nature* **174**, 1057 (1954)] was isolated essentially as described (*7*). Wood was first ground in a Wiley mill (1-mm screen), and soluble phenolics, carbohydrates, and other components were removed by successive extractions with diethyl ether, acetone, methanol, and water. Wood from the mutant had more extractable colored material than did the normal wood, with substantial amounts of coniferaldehyde and vanillin (*19*). Six cycles of acetone and water extractions removed most of the colored material. Klason lignin [R. D. Hatfield, H. G. Jung, J. Ralph, D. R. Buxton, P. J. Weimer, *J. Sci. Food Agric.* **65**, 51 (1994)] levels were 32% (w/w) for the *cad-n1* mutant and 31% for the normal wood. The ground wood was then ball-milled and extracted with 96:4 dioxane:water. Saccharides and metal ions were removed with EDTA (*7*). The final yields of milled wood lignin were 12.5% of the lignin in normal pine and 17% in the *cad-n1* mutant; Klason lignin contents were 93% by weight for each, total carbohydrates were ~2% each, and total uronosyls were 2 to 5%.
21. Vanillin is produced from coniferaldehyde by an aldol reaction that can occur at neutral pH (*2*).
22. Long-range C-H correlation NMR experiments (not shown) establish that a correlated oxygenated aromatic carbon is within three bonds of the methoxyl protons and the aldehyde proton. These correlations are only possible from 2-methoxybenzaldehydes.
23. L. Lerner and A. Bax, *J. Magn. Reson.* **69**, 375 (1986). HMQC-TOCSY ^{13}C-^{1}H correlation spectra are particularly valuable because all carbons and protons within a coupling network (for example in a lignin unit side chain) correlate with each other (although correlation intensities depend on coupling constants and other factors), providing information on the nature of these units. HMQC-TOCSY spectra of samples (~80 mg) in 9:1 acetone-d_6:D_2O were obtained with the unmodified Bruker "invbmltp" pulse program for phase-sensitive inverse-detected C-H correlation with the use of a BIRD sequence for minimizing protons bound to ^{12}C-carbons (300-ms inversion-recovery delay) and MLEV-17 Hartman-Hahn mixing (100 ms) with a Bruker AMX-360 360-MHz narrow-bore instrument. Other acquisition parameters: spectral widths, 11.7 ppm (^{1}H) and 212 ppm (^{13}C); acquisition time, 0.243 s; relaxation delay, 1 s; 256 increments of 200-scan 2 K free induction decays. Processing: optimized Gaussian apodization (LB = −2, GB = 0.01) in t_2 and cosine-squared bell apodization in t_1, phase-sensitive (TPPI) Fourier transform with zero-filling to 1 K by 1 K real data points resulting in 4.1 (^{1}H) and 18.6 (^{13}C) Hz/pt digital resolutions.
24. NMR data for model compounds, dihydroconiferyl alcohol moiety side chain resonances only. Model **8a**, 1-(4-hydroxy-3-methoxyphenyl)-2-[4-(3-hydroxypropyl)-2-methoxy-phenoxy]-propane-1,3-diol, the β-ether cross-product of coniferyl alcohol and dihydroconiferyl alcohol: NMR (acetone-d_6): δ_C/δ_H: 32.6/2.60 (α), 35.9/1.78 (β), 61.7/3.55 (γ). Model **8b**, 4-[3-hydroxymethyl-5-(3-hydroxypropyl)-7-methoxy-2,3-dihydrobenzofuran-2-yl]-2-methoxyphenol, the phenylcoumaran (β-5) cross-product of coniferyl alcohol and dihydroconiferyl alcohol: NMR (acetone-d_6): δ_C/δ_H: 32.4/2.61 (α), 35.6/1.78 (β), 61.7/3.54 (γ). Model **8c**, di-(3-hydroxypropyl)-*trans*-6,7-dihydro-7-(4-hydroxy-3-methoxyphenyl)-4,9-dimethoxy-dibenzo[e,g][1,4]dioxocin-6-yl methanol, the 5-5-coupled dimer of dihydroconiferyl alcohol then coupled 4-*O*-β to coniferyl alcohol to form a dibenzodioxocin [P. Karhunen, P. Rummakko, J. Sipilä, G. Brunow, I. Kilpeläinen, *Tetrahedron Lett.* **36**, 169 (1995)]: NMR (acetone-d_6): δ_C/δ_H: 32.81,32.85/

2.70,2.74 (α), 35.58,35.67/1.85,1.89 (β), and 61.78,61.84/3.60 (γ).
25. S. Quideau and J. Ralph, *J. Agric. Food Chem.* **40**, 1108 (1992); F. H. Ludley and J. Ralph, *ibid.* **44**, 2942 (1996).
26. J. Ralph, R. F. Helm, S. Quideau, R. D. Hatfield, *J. Chem. Soc. Perkin Trans.* **1**, 2961 (1992). The synthetic lignin was prepared by slow addition of solutions of [$O^{12}C^2H_3$]-coniferyl alcohol and hydrogen peroxide to a buffered solution of horseradish peroxidase. The isotopic labeling in the coniferyl alcohol was done to reduce the impact on NMR spectra of the normally intense methoxyl peaks.
27. R. A. Savidge, *Phytochemistry* **26**, 93 (1987).
28. S. Kamisaka, N. Sakurai, K. Shibata, *Plant Cell Physiol.* **24**, 369 (1983).
29. We made these determinations by analyzing monomers released after cleaving all α- and β-ethers in the lignin by the DFRC method (derivatization followed by reductive cleavage) (F. Lu and J. Ralph, *J. Agric. Food Chem.*, in press), which gives data analogous to analytical thioacidolysis [C. Lapierre, in *Forage Cell Wall Structure and Digestibility*, H. G. Jung, D. R. Buxton, R. D. Hatfield, J. Ralph, Eds. (American Society of Agronomy, Madison, WI, 1993), pp. 133–166; C. Rolando, B. Monties, C. Lapierre, in *Methods in Lignin Chemistry*, C. W. Dence and S. Y. Lin, Eds. (Springer-Verlag, Berlin, Heidelberg, 1992), pp. 334–349]. Dihydroconiferyl peracetate (*m/z* 266) was abundant. There was no difference between the mutant and the normal pine for the small amounts of dihydro-*p*-coumaryl acetates (*m/z* 236).
30. L. B. Davin *et al.*, *Science* **275**, 362 (1997).
31. J. Ralph *et al.*, in *Lignin and Lignin Biosynthesis*, N. G. Lewis and S. Sarkanen, Eds. (American Chemical Society, Washington, DC, in press); J. Ralph, J. H. Grabber, R. D. Hatfield, *Carbohydr. Res.* **275**, 167 (1995).
32. C. Lapierre, M. T. Tollier, B. Monties, *C. R. Acad. Sci. Ser. 3* **307**, 723 (1988).
33. B. Monties, *Ann. Proc. Phytochem. Soc.* **5**, 161 (1995).
34. We are grateful to F. Lu for providing analytical data obtained by DFRC, which verified the NMR findings and provided data on the high *p*-coumaryl alcohol component; to Y. Zhang for preparing the synthetic lignin; to S. Ralph, L. Landucci, and F. Ludley for help in lignin preparation steps and model work on the coniferaldehyde components; and to J. Grabber for valuable input. NMR studies at 750 MHz for supporting data were carried out at the National Magnetic Resonance Facility at Madison, WI. Samples were provided from a Westvaco planting containing selfs of 7-56 by L. Pearson (Westvaco, Summerville, SC) and G. Askew (Baruch Experimental Forest, Clemson University, Georgetown, SC). We are grateful for partial funding from the U.S. Department of Agriculture–National Research Initiatives, Plant Growth and Development section (grants 94-02764 and 96-02587), and for grants from NIH (GM45344-07), U.S. Department of Energy (DE-FG05-92ER20085), and the NCSU Forest Biotechnology Industrial Research Consortium.

18 February 1997; accepted 27 May 1997

Coding the Locations of Objects in the Dark

Michael S. A. Graziano,* Xin Tian Hu, Charles G. Gross

The ventral premotor cortex in primates is thought to be involved in sensory-motor integration. Many of its neurons respond to visual stimuli in the space near the arms or face. In this study on the ventral premotor cortex of monkeys, an object was presented within the visual receptive fields of individual neurons, then the lights were turned off and the object was silently removed. A subset of the neurons continued to respond in the dark as if the object were still present and visible. Such cells exhibit "object permanence," encoding the presence of an object that is no longer visible. These cells may underlie the ability to reach toward or avoid objects that are no longer directly visible.

A scientist sitting in her office reaches for a book on the shelf. She knows where the book is located and does not need to look in order to guide her hand. Later, while driving home, she adjusts the car radio while her eyes are fixed on the road. That night, in darkness, she reaches toward a box of tissues on the bedside table. How does the brain keep track of the locations of objects that are no longer in sight, and how does it guide movements toward or away from those objects? Piaget (*1*) was the first to emphasize the importance of object permanence, that is, the knowledge that an object is still present even though it is no longer visible. More recently, researchers have emphasized the more specific problem of how movements toward these unseen objects are guided (*2*). Here we describe visually responsive neurons in the ventral premotor cortex (PMv) of the monkey brain that appear to solve the problem of object permanence. These neurons keep track of the locations of objects near the monkey's body, even after the lights are turned off and the monkey is in darkness.

PMv, the area of cortex just posterior to the lower limb of the arcuate sulcus, is thought to be involved in the sensory guidance of movement (*3*). Its neurons respond to tactile and visual stimuli and also during movements of the head and the arms (*4*). About 40% of the neurons in PMv have both a tactile and a visual receptive field (RF). For these bimodal cells, the visual RF extends from the approximate region of the tactile RF into the immediately adjacent space (Fig. 1). For most cells with a tactile RF on the arm, when the arm moves, the visual RF moves with it, and for most cells with a tactile RF on the face, when the head is rotated, the visual RF moves with it (*5*). In contrast, when the eyes move, the visual RFs do not move but remain anchored to the body surface (*5*, *6*). These visual RFs, therefore, encode the locations of nearby stimuli relative to different parts of the body. One suggestion is that the bimodal neurons help to guide movements of the head and arms toward or away from nearby stimuli (*7*).

We tested whether the bimodal neurons in PMv encode the locations of nearby stimuli that are no longer visible. Responses of single neurons in PMv were studied in two tame male *Macaca fascicularis* (4.6 and 5.0 kg). For details of the experimental procedures, see (*5*). Daily recording sessions were conducted on each monkey while the animal was seated in a primate chair with the head fixed. A hydraulic microdrive was used to lower an electrode into PMv. Once a neuron was isolated, it was tested for somatosensory and visual responsiveness. Somatosensory RFs were plotted by manipulating the joints and stroking the skin, and visual RFs were plotted with objects presented on a wand. In addition, we made the unexpected observation that neurons with a tactile RF extending onto the back of the head often responded to auditory stimuli; therefore, we also routinely tested for auditory responsiveness.

Of 153 isolated single neurons, 6 (4%) responded only to visual stimuli, 34 (22%) responded only to somatosensory stimuli, 55 (36%) were bimodal, responding to visual and tactile stimuli, and 11 (7%) were tri-

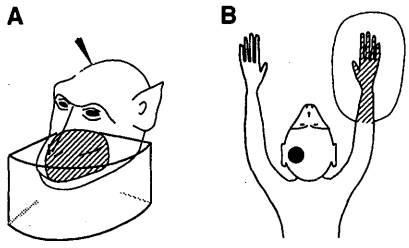

Fig. 1. Receptive fields of two bimodal, visual-tactile neurons in PMv. (**A**) The tactile RF (shaded) is on the snout, mostly contralateral to the recording electrode (indicated by the arrowhead) but extending partially onto the ipsilateral side of the face. The visual RF (boxed) is contralateral and confined to a region of space within ~10 cm of the tactile RF. (**B**) The tactile RF for this neuron is on the hand and forearm contralateral to the recording electrode (indicated by the black dot), and the visual RF (outlined) surrounds the tactile RF.

Department of Psychology, Princeton University, Princeton, NJ 08544, USA.

*To whom correspondence should be addressed. E-mail: graziano@princeton.edu